

Electrically Tunable Absorption in Graphene-Integrated Silicon Photonic Crystal Cavity

Leili Abdollahi Shiramin¹, Weiqiang Xie¹, Brad Snyder², Peter De Heyn², Peter Verheyen², Gunther Roelkens¹, Dries Van Thourhout¹

¹Photonics Research Group, Ghent University-IMEC, Technologiepark-Zwijnaarde 15, Ghent 9052, Belgium

²imec, Kapeldreef 75, 3001 Leuven, Belgium

E-mail address: leili.abdollahishiramin@ugent.be

Abstract—We demonstrate 17 dB extinction ratio in an electrically gated graphene-integrated silicon photonic crystal cavity by applying -1.2 V gate voltage. The shift of resonance wavelength for the same voltage range is 0.75 nm. The size of the graphene layer is only 5 μm^2 .

I. Introduction

Since graphene's fermi level can be tuned by applying an electric field [1,2], it is an attractive candidate for light modulation. Several waveguide integrated graphene devices have already been studied, both theoretically and experimentally [3-8]. However, when integrated on straight waveguides, the graphene layer should be sufficiently long to achieve a high extinction ratio (ER). Integrating graphene with resonant structures such as photonic crystal (PhC) cavities enhances the interaction of the optical field with the graphene layer [9,10] and strongly reduces the required graphene length. As a consequence the device capacitance and the power consumption under high speed modulation will be considerably reduced. In this work, we investigate the impact of the fermi level shift on the transmission of a graphene integrated 1D PhC through ion gel gating.

II. Fabrication

An array of 1-D PhC nano-cavities integrated with grating couplers were fabricated on a 300 mm SOI wafer in a CMOS pilot line using 193 nm immersion lithography. Micron sized CVD graphene layers protected by resist were then transferred on the cavity with an automated commercial transfer printer, X-Celeprint, model $\mu\text{TP-100}$, (see [11] for more details). After cleaning the transferred graphene, palladium contact pads were fabricated on both sides of the graphene layer. The second contact is required only for characterizing the graphene sheet resistance. Finally, a polymer electrolyte consisting of a mixture

LiClO₄:PEO in a weight ratio 1:10 is spin-coated on the sample. Figure 1 is the image of the sample after fabrication.

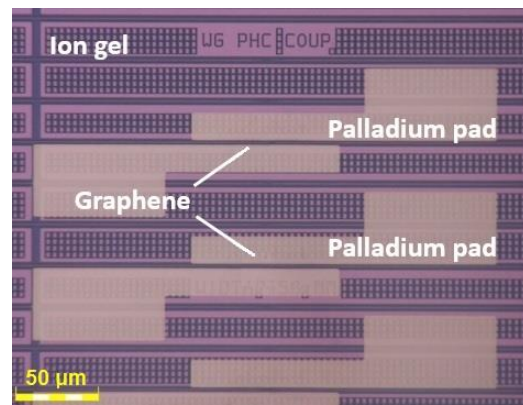


Fig. 1. The fabricated device, showing graphene on the PhC cavity and palladium pads in both side of graphene. Ion gel is coated on the sample after metal pads lift-off.

III. Characterization

A CW laser is coupled in and out of the waveguide through grating couplers. The graphene fermi level is tuned by applying a gate voltage V_{gs} between one of the contacts of the device under study and a contact of an identical device directly next to it. The neutrality point is determined by measuring the gate voltage dependent resistance R_{DS} of the device under study. The neutrality point is found at 0.8 Volt, equivalent with a chemical potential $\mu_c = 0.1$ eV.

Figure 2.a plots the spectrum of a cavity for different applied gate voltages. Starting from the neutrality point at 0.8 Volt, the transmission increases as the voltage becomes more negative. This indicates the graphene layer becomes more transparent, as expected. For positive voltages this effect is weaker as the transferred graphene is intrinsically p-doped. As can be seen from Figure 2.b, applying only -1.2 Volt results already in an extinction ratio (ER) as

high as 17.2 dB. With increasing the drive voltage to 2 Volt, from -1.2 to 0.8 Volt (the neutrality point of graphene), the ER further increases to 19dB.

The gate voltage dependent quality factor is extracted by fitting a Lorentzian function to the transmission spectra. It increases from 900 at 0.8 Volt to about 1800 at -1.2 Volt. The shift of the resonance wavelength for the same voltage range is 0.8 nm (Figure 3). This strong blue shift with decreasing voltage indicates there is not only a strong modulation of the imaginary part of graphene's refractive index but also of its real part, resulting in a phase shift. In line with what is expected from theory, this change in the real part is in particular relevant if the chemical potential comes close to 0.4eV, or for gate voltages below 0 Volt.

The shift of the cavity resonance and its line width vary linearly with the gate-dependent dielectric constant of graphene. The theoretical fits in Figure 3 are obtained as $\Gamma_R = \Gamma_R^0 + \alpha \text{Im}[\epsilon_g(\omega)]$ for the cavity line width and $\lambda_R = \lambda_R^0 + \beta \text{Re}[\epsilon_g(\omega)]$ for the cavity resonance wavelength [10]. The theoretical Q factor is then calculated from the line width and cavity resonance.

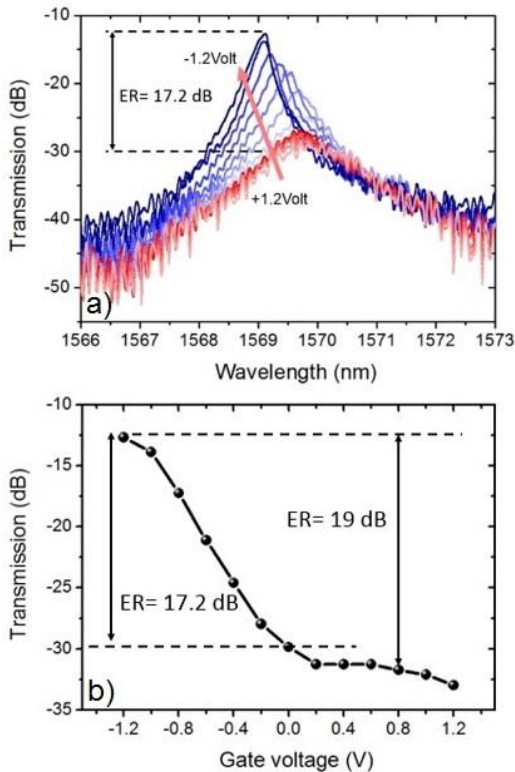


Fig. 2. a) The transmission of the device versus wavelength for different gate voltages. b) The transmission versus gate voltage, showing the ER.

The size of the graphene covering the 1D PhC ($1\mu\text{m} \times 5\mu\text{m}$) is very small compared to most earlier demonstrated devices. This opens prospects for high speed modulation and low power consumption.

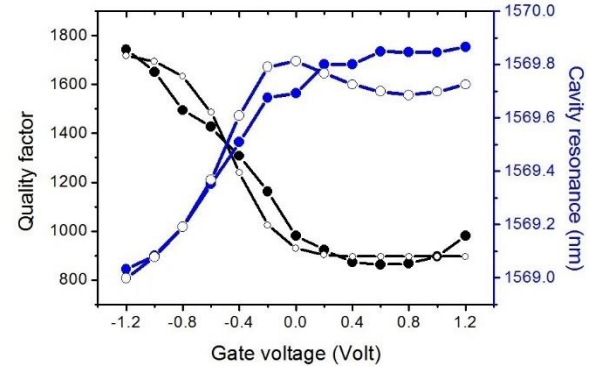


Fig. 3. The quality factor and cavity resonance versus gate voltage. Open and solid circles indicate the theoretical and experimental data, respectively.

IV. Conclusion

In summary, we demonstrated a graphene based switch exhibiting an ER of 17 dB for an applied gate voltage of only -1.2 Volt. The size of the graphene layer is only $1\mu\text{m} \times 5\mu\text{m}$, showing the strong potential for realizing compact high speed electro-optical modulators. To broaden the optical bandwidth of the device, a coupled cavity design optimized for achieving a flat passband could be designed.

Acknowledgment

We acknowledge support by the EU commission through the Graphene Flagship and TOPHIT projects. This work was supported by imec's industry-affiliation program on Optical I/O. We thank Prof. Daniel Neumaier and Dr. Muhammad Mohsin for providing the polymer electrolyte.

References

- [1] A. Neto et al., *Rev. Mod. Phys.*, **81**, (2009)
- [2] A. Rozhkov, *Phys. Rep*, **648**, (2016).
- [3] L. A. Shiramin et al., *JSTQE*, **23**, (2017).
- [4] V. Soriano et al., *Opt.ex*, **23**, (2015)
- [5] Y. Hu et al., *LPR*, (2016).
- [6] H. Dalir, et al, *ACS Photonics*, **3**, (2016).
- [7] M. Liu, et al., *Nature*, **474**, (2011).
- [8] M. Liu, et al., *Nano lett*, **12**, (2012).
- [9] A. Majumdar et al., *Nano. lett*, **13**, (2013).
- [10] X. Gan et al., *Nano. lett*, **13**, (2013).
- [11] L. A. Shiramin et al., *CLEO*, (2017).